Aleksandar Stefanović
Research Assistant
University of Belgrade
Faculty of Mechanical Engineering

Nebojša Gnjatović
Assistant Professor
University of Belgrade
Faculty of Mechanical Engineering

Goran Milojević
Research Assistant
University of Belgrade
Faculty of Mechanical Engineering

Stevan Đenadić
Teaching Assistant
University of Belgrade
Faculty of Mining and Geology

Marko Urošević
Research Assistant
University of Belgrade
Faculty of Mechanical Engineering

Analysis of the impact of the frequency-controlled bucket wheel drive on the dynamic response of the excavator superstructure

Bucket wheel excavators (BWEs) are the largest mobile terrestrial machines exposed to the working loads of a periodic character. This paper presents a small portion of the studies, conducted with the goal of proposing a new idea regarding preservation of the load-carrying structures of these machines, based on the implementation of a controllable frequency-controlled drive of the excavating device. A detailed analysis of the dynamic response of the load-carrying structure is required in order to determine the domains of frequency of revolutions of the working device's driving motor where the dynamic response of the structure is favorable, and therefore successfully implement this idea. A methodologically-original study was conducted, using a unique dynamic model of the BWE slewing superstructure that allows for the continuous variation of the frequency of excitation. This has yielded the resonant-free domains, i.e. the domains where the structure is not exposed to the excessive dynamic impacts.

Keywords: *bucket wheel excavator, slewing superstructure, structural helth, dynamic response, frequency-controlled drive*

1. INTRODUCTION

Continuous earthmoving machines, such as bucket wheel excavators (BWEs) [1,2], Fig. 1, represent the largest mobile terrestrial machinery [3] and the backbone of surface mining systems. Currently, there is a strong trend towards their revitalization and modernization [4,5], along with increasing the degree of reliability [6–8] and safety [9,10], reducing financial losses caused by downtimes [11,12], and prolonging their operational life. These procedures include the mechanical and electrical equipment, while the existing load-carrying structure is preserved. For this reason, extensive numerical-experimental studies aimed at ensuring the durability of load-carrying structures [4] accompany the revitalizations of BWEs.

Figure 1. The bucket wheel excavator SchRs 1600 on the surface mine 'Tamnava West Field' (Serbia): theoretical capacity of 6600 m³/h, total mass (with the discharge bridge and loading unit) of 3344 t.

BWEs operate in exceptionally harsh exploitational conditions, as they are under constant exposure to the loads of a pronounced dynamic character in a 24/7 working regime. The periodic character of the loads, i.e. loads caused by the forces resisting the excavation, is primarily caused by the periodic, enter-exit, interaction between the soil and the buckets [13,14]. As such, the dynamic response of the load-carrying structure of this class of earthmoving machines is dominantly affected by the loads caused by the forces which resist the excavation. As for the low-frequency oscillations, the dominant impact is that of the slewing superstructure, the most flexible portion of the entire load-carrying structure of the machine. For the above-stated reasons, the studies presented herein deal with the dynamic response of the slewing superstructure of the BWE SchRs 1600 to the periodic excitation caused by the forces resisting the excavation, under the conditions of a variable motor revolution at the frequency-controlled bucket wheel drive.

Currently, frequency controllers of the bucket wheel drive are being used to protect the drive itself and in order to adapt the machine to the properties of the working environment. Namely, a reduced number of the bucket wheel revolutions results in an increased moment of excavation, allowing the machine to excavate soils of higher strength. The primary idea which led to the studies presented in this paper is to control the frequency controller of the bucket wheel drive in a way that passes over certain numbers of bucket wheel revolutions, thus not only avoid the potential resonant states of the slewing superstructure but also avoid the states that are in their close proximity (resonance affected states: RAS) which, over a multidecadal exploitation, inevitably cause the fatigue cracks to appear [4,15–17]. In such a manner and based on the predetermined working regimes, the system controlling the working process would allow the slewing superstructure to avoid these undesired states, while

Correspondence to: Aleksandar Stefanović, research assistant
Faculty of Mechanical Engineering,
Kraljice Marije 16, 11120 Belgrade 35, Serbia
E-mail: astefanovic@mas.bg.ac.rs

leaving all of the existing protection systems of a bucket wheel excavator intact. Even though the results of the studies highlight the problem of resonance of the load-carrying structure in BWEs and a clear need for the calculation-based identification of the potential resonant states [4,18–21], the existing technical regulations, i.e. standards [22–24], do not impose a requirement for a mandatory calculation of the dynamic response of the structure [25]. Only the standard [23] mentions the need for determining the possible resonant excitation, but provides no procedures nor criteria for assessing the proximities of the RAS. In BWEs, as already known, the fundamental frequency of excitation caused by the forces resisting excavation depends on the two crucial parameters of the excavating device - it is proportional to the the bucket wheel frequency of revolution and the number of buckets on the bucket wheel. The impact of the number of buckets on the dynamic behavior of the slewing superstructure of a BWE, under the nominal frequency of the bucket wheel revolution, is analyzed in detail in [26]. Below is presented a study on the impact of the bucket wheel frequency of revolution of the dynamic behavior of the slewing superstructure of a BWE as a foundation for the implementation of the proposed idea which, simultaneously and fully, both operatively and methodologically, solves the problem of selection of key parameters of the excavating device of a BWE and their impact on the dynamic response of its slewing superstructure.

Successful realization of the idea to preserve the structural health of a BWE using a frequency-controlled bucket wheel drive calls for determination of ranges of the bucket wheel revolution frequencies where the vibroactivity of the load-carrying structure is within the allowed boundaries. For the purposes of the studies presented in this paper, they were determined on the basis of limiting accelerations of the referent points of the slewing superstructure of the BWE, prescribed by the German standard DIN 22261-2 [22]. This should not be seen as a limitation of the presented method, as it can be successfully applied to other types of continuous earthmoving machines (bucket chain excavators, bucket wheel reclaimers, and reclaimers), stackers, as well as load-carrying structures of various uses which are exposed to the periodically-variable working loads and at the risk of potentially entering the RAS.

2. SPATIAL DYNAMIC MODEL

A research on the impact of the bucket wheel frequency of revolution, i.e. the frequency of revolution of the bucket wheel drive electromotor (FREM), on the dynamic response of the referent points of the structure, determined in accordance with the standard [22], was conducted using a spatial reduced dynamic model of the slewing superstructure with 64 degrees of freedom, created for the BWE SchRs 1600, Fig.2. The procedure for the formation and validation of the model, which has already been successfully applied for the analysis of the impacts of the number of buckets [26], the counterweight mass [27], as well as incrustation and chute blockage [28] on the dynamic response of the structure, is presented in detail in [29].

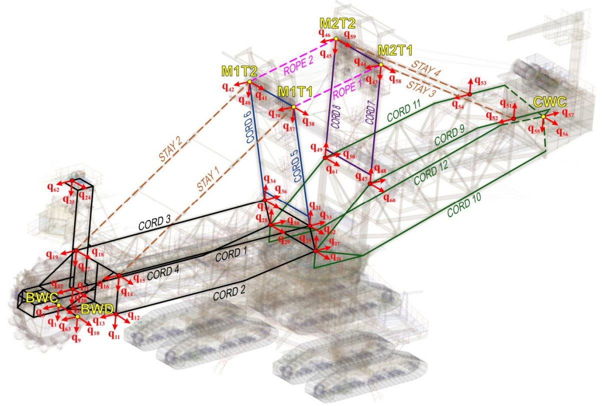

Figure 2. Referent points of the spatial reduced dynamic model of the slewing superstructure of the BWE SchRs 1600 [29]: BWC-bucket wheel center; BWD-center of gravity of the gearbox of the bucket wheel drive; M1T1-Mast 1, Tip 1; M1T2-Mast 1, Tip 2; M2T1-Mast 2, Tip 1; M2T2-Mast 2, Tip 2; CWC-counterweight center of gravity.

The frequency of the fundamental harmonic of excitation, caused by the resistance to excavation, is determined in accordance with the expression [30]

$$f_{e,1} = n_B n_{BW}, \tag{1}$$

where n_B=17 is the total number of buckets on the bucket wheel and n_{BW} is the frequency of the bucket wheel revolution, determined as

$$n_{BW} = \frac{n_m}{i_{BWD}}, \tag{2}$$

where: n_m is the FREM and i_{BWD}=255.363 is the ratio of the bucket wheel drive gearbox.

Given that the first order resonances have the highest impact on the dynamic behavior of the structure, the remainder of the analysis considers only the impact of the excitation loads developed up to the first member of the Fourier series, determined under the assumption that the excavation process is conducted employing the total nominal power of the bucket wheel drive ($P_{BWD,nom}$=1150 kW).

3. RESULTS

The nominal FREM at the analyzed BWE is $n_{m,nom}$=1000 rpm. In continuation of the research, the FREM was varied over a continuous domain with the range between 600 rpm and 1000 rpm, in accordance with the parameters of the bucket wheel drive gearbox. The frequencies of the first excitation harmonic correspond to the outlined FREM boundaries and were determined with the Eq. (1). The highest frequency of the frst harmonic of excitation, $f_{e,\max}$=1.110 Hz, is lower than the 4[th] natural frequency of the model (f_4=1.562 Hz). In the considered case, the intersection between the infinite set of the first harmonic of excitation and the finite set of the first 3 natural frequencies of the model contains a total of 3 elements, Fig. 3, which means that 3 resonant states might occur in the low frequency area (up to 1.25 Hz). The resonant FREMs ($n_{m(Rj)}$ j=1,2,3), Table 1, were determined by equaling the frequency of the first harmonic of excitation ($f_{e\,(j)}$), Eq. (3), which causes the j-

th resonant state, Fig. 3, and the frequency of the $i(j)$-th mode of the dynamic model ($f_{i(j)}$), excited in the j-th resonant state Fig. 3

$$n_{\mathrm{m(Rj)}} = \frac{i_{\mathrm{BWD}}}{n_{\mathrm{B}}} f_{\mathrm{i(j)}}, \quad i(j) = 1, 2, 3. \qquad (3)$$

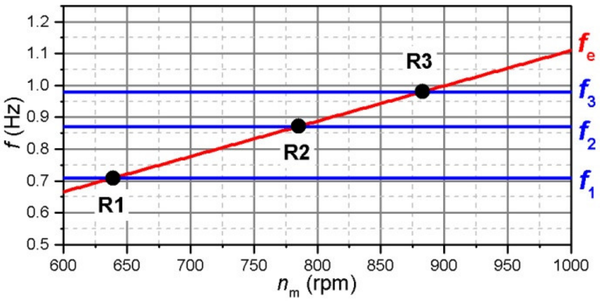

Figure 3. A comparative display of the natural frequencies (blue lines) and frequency of the first harmonic of excitation (red line): Rj, j=1,2,3 is the index of the resonant state.

Table 1. The resonant FREMs

Resonant state	Resonant FREM (rpm)
R1	638.842
R2	785.215
R3	882.897

Considering that a comparative analysis of the natural frequencies of the dynamic model and the frequency of the first harmonic of excitation does not provide insight into the widths of the resonant areas and that the referent literature from the field of BWE design provides no recommendations which would lead to the determination of the widths of the resonant areas, the limiting (permissible) accelerations of the referent points of the slewing superstructure prescribed by the relevant German standard DIN 22261-2 [22], Table 2, were adopted as the basis for determining the FREM resonant domains, i.e. the widths of the resonant areas.

Table 2. Limiting vertical ($a_{\mathrm{V,per}}$) and lateral ($a_{\mathrm{L,per}}$) accelerations of the referent points

Referent point	Limiting accelerations (m/s^2)	
	vertical ($a_{\mathrm{V,per}}$)	lateral ($a_{\mathrm{L,per}}$)
BWC	1.5	0.25
BWD		
M1T1	0.4	0.333
M1T2		
M2T1		
M2T2		
CWC		

Based on the cut-off scanning of the responses (maximal intensities of accelerations) of the referent points of the slewing superstructure to the first harmonic of excitation, Figs. 4–15, the boundaries of the FREM resonant domains were determined: the lower limit is $n_{\mathrm{m,Rj,LL}}$ and the upper limit is $n_{\mathrm{m,Rj,UL}}$, j=1,2,3, Tables 3–8. In Figs. 4–15 the zones of excessive accelerations are grey colored.

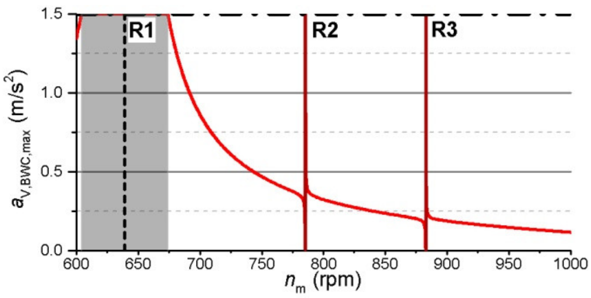

Figure 4. Maximal vertical accelerations of the BWC.

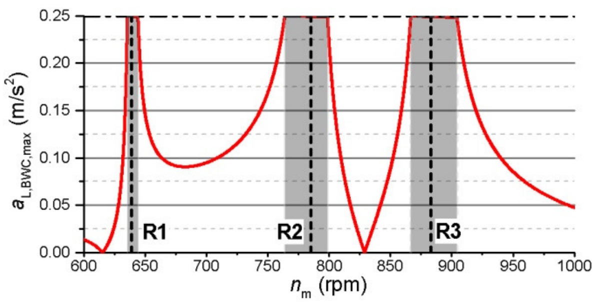

Figure 5. Maximal lateral accelerations of the BWC.

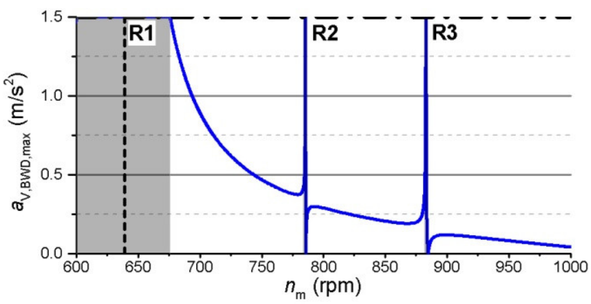

Figure 6. Maximal vertical accelerations of the BWD.

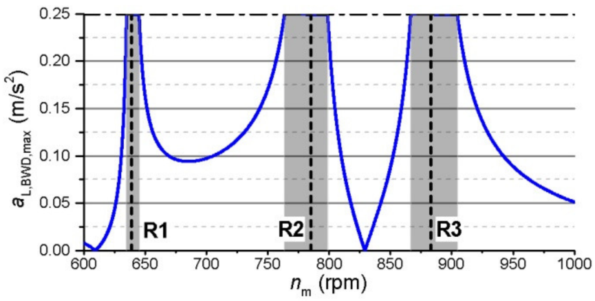

Figure 7. Maximal lateral accelerations of the BWD.

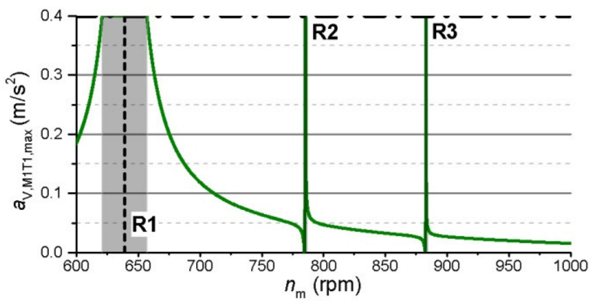

Figure 8. Maximal vertical accelerations of the M1T1.

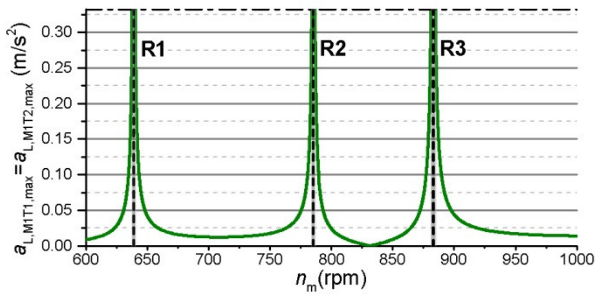

Figure 9. Maximal lateral accelerations of the M1T1 and M1T2.

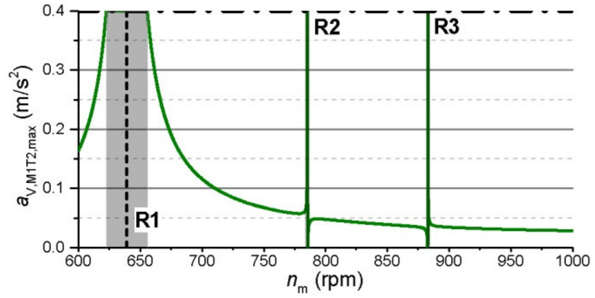

Figure 10. Maximal vertical accelerations of the M1T2.

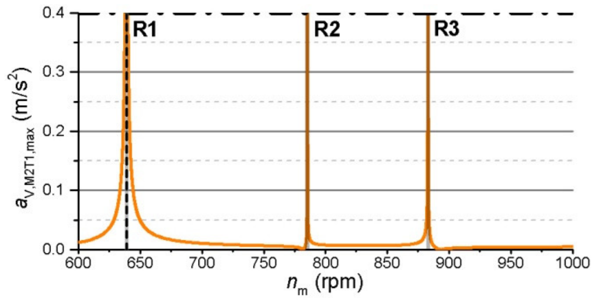

Figure 11. Maximal vertical accelerations of the M2T1.

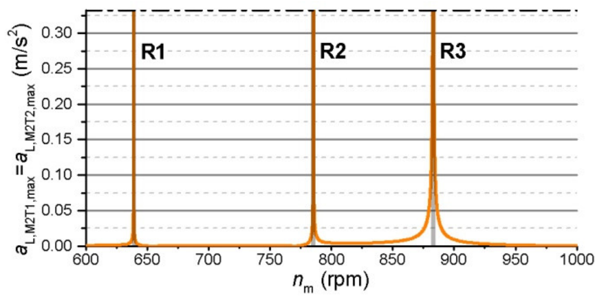

Figure 12. Maximal lateral accelerations of the M2T1 and M2T2.

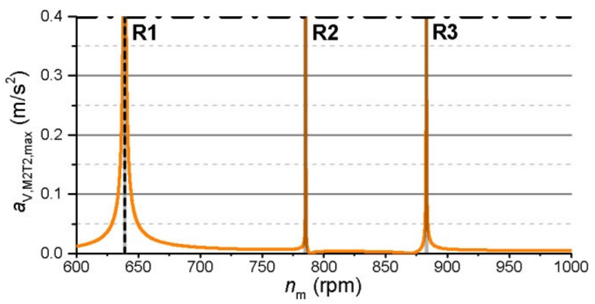

Figure 13. Maximal vertical accelerations of the M2T2.

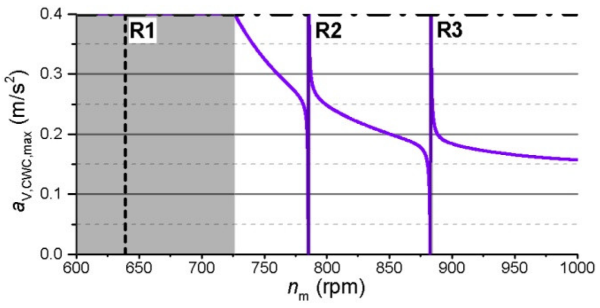

Figure 14. Maximal vertical accelerations of the CWC.

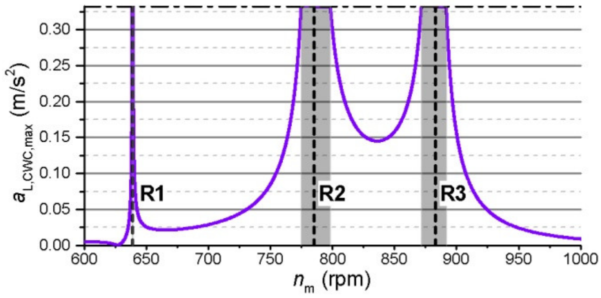

Figure 15. Maximal lateral accelerations of the CWC.

Table 3. Boundaries of the FREM resonant domains according to $a_{V,per}$: resonance R1

Referent point	$n_{m,R1,V,LL}$	$n_{m,R1,V,UL}$
	rpm	
BWC	604.000	674.003
BWD	600.594	675.812
M1T1	620.781	657.031
M1T2	622.508	655.789
M2T1	637.529	640.170
M2T2	637.527	640.172
CWC	**600.000**	**726.406**

Table 4. Boundaries of the FREM resonant domains according to $a_{V,per}$: resonance R2

Referent point	$n_{m,R2,V,LL}$	$n_{m,R2,V,UL}$
	rpm	
BWC	785.178	785.247
BWD	785.106	785.284
M1T1	785.114	785.344
M1T2	785.168	785.251
M2T1	785.160	785.271
M2T2	785.167	785.262
CWC	785.100	785.764

Table 5. Boundaries of the FREM resonant domains according to $a_{V,per}$: resonance R3

Referent point	$n_{m,R3,V,LL}$	$n_{m,R3,V,UL}$
	rpm	
BWC	882.868	882.935
BWD	882.692	883.063
M1T1	882.847	882.953
M1T2	882.872	882.926
M2T1	882.765	883.025
M2T2	882.756	883.040
CWC	882.741	883.323

Table 6. Boundaries of the FREM resonant domains according to $a_{L,per}$: resonance R1

Referent point	$n_{m,R1,L,LL}$	$n_{m,R1,L,UL}$
	rpm	
BWC	635.389	644.045
BWD	634.726	645.008
M1T1	637.560	640.153
M1T2	638.807	638.880
M2T1	638.460	639.258

Table 7. Boundaries of the FREM resonant domains according to $a_{L,per}$: resonance R2

Referent point	$n_{m,R2,L,LL}$	$n_{m,R2,L,UL}$
	rpm	
BWC	763.670	798.764
BWD	**763.438**	**798.906**
M1T1	783.837	786.548
M1T2	785.127	785.304
M2T1	774.578	798.328

Table 8. Boundaries of the FREM resonant domains according to $a_{L,per}$: resonance R3

Referent point	$n_{m,R3,L,LL}$	$n_{m,R3,L,UL}$
	rpm	
BWC	866.650	904.150
BWD	**866.594**	**904.531**
M1T1	881.073	884.815
M1T2	882.370	883.421
M2T1	871.644	891.676

4. DISCUSSION

Over the considered FREM domain (600 rpm≤n_m≤1000 rpm), three resonances of the first order (R1, R2 and R3) might occur, Table 1, Fig. 3.

Resonance R1 is caused by the first harmonic of excitation, Fig. 3, at $n_{m(R1)}$=638.842 rpm, Table 1. The maximal vertical accelerations of the referent points are significantly more sensitive to the occurrence of the first order resonance than their maximal lateral accelerations, Tables 3–8, which was to be expected having in mind the fact that the oscillations of the system in the vertical plane are dominant in the first mode, Fig. 16. Resonance R1 has the biggest impact on the values of the maximal vertical accelerations of the counterweight center of gravity (CWC). Namely, the criterion of limiting vertical accelerations was not satisfied over the domain from $n_{m,R1,LL}$=$n_{m,R1,V,LL,CWC}$=600 rpm to $n_{m,R1,UL}$=$n_{m,R1,V,UL,CWC}$=727 rpm, Table 3, Fig. 14. The impact of the resonance R1 is also noticeable on the diagrams of maximal vertical accelerations of the bucket wheel center (BWC) and the bucket wheel drive gearbox center of gravity (BWD), Figs. 4 and 6, where the FREM domains which do not meet the criterion of limiting vertical accelerations are 604 rpm≤n_m≤675 rpm and 600 rpm≤n_m≤676 rpm, respectively, Table 3.

Resonances R2 and R3 are also caused by the first harmonic of excitation, Fig. 3, at $n_{m(R2)}$=785.215 rpm and $n_{m(R3)}$=882.897 rpm, respectively, Table 1. In the second and third modal shape, the dominant form of deformation of the slewing superstructure is in the horizontal plane, Figs. 17 and 18, which is why the maximal lateral accelerations of the referent points of the system are significantly more sensitive to the appearances of resonances R2 and R3 than the maximal vertical accelerations, Figs. 4–15.

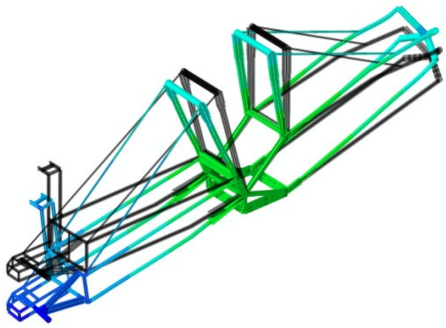

Figure 16. The first modal shapes of the slewing superstructure.

Maximal lateral accelerations of the bucket wheel center (BWC) and the bucket wheel drive gearbox center of gravity (BWD) are almost equally sensitive to the appearance of the resonance R2, Figs. 5 and 7, and, therefore, the FREM range of 763 rpm≤$n_{m,R2}$≤799 rpm can be adopted as the width of this resonant area, Table 7. As for the resonance R3, the most sensitive values are those of the maximal lateral accelerations of the center of gravity of the bucket wheel drive gearbox (BWD), Fig. 7 and Table 8. The FREM width of the R3 resonant area was determined on the basis of the criterion of limiting lateral accelerations of this referent point, and equals 866 rpm≤$n_{m,R3}$≤905 rpm, Table 8.

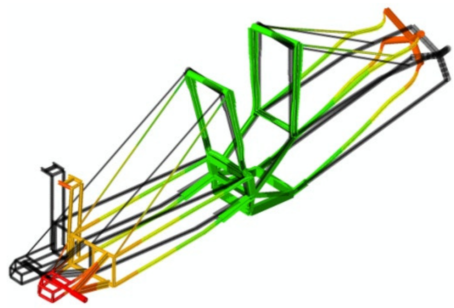

Figure 17. The second modal shapes of the slewing superstructure.

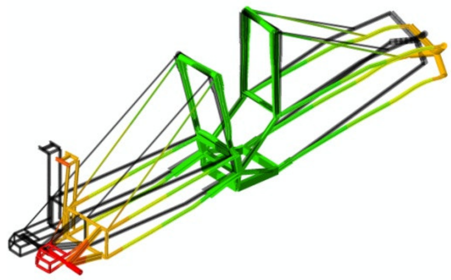

Figure 18. The third modal shapes of the slewing superstructure.

Based on the presented results, it can be concluded that the slewing superstructure has the highest sensitivity to the appearance of the resonance R1, which was to be expected. The upper limit of the FREM domain where the criteria prescribed by the standard DIN 22261-2 have not been met is located within the defined span of frequency regulation: $n_{m,R1,UL}$=727 rpm, Fig. 14. Being a resonance of the first order, which occurs when the first

natural frequency crosses the first frequency of excitation, in order to determine the real width of the resonant area, the span of frequency regulation was conditionally expanded, and, instead of 600 rpm, the value of 500 rpm was adopted as the hypothetical lower limit of the span. Based on the criterion of limiting vertical accelerations of the center of gravity of the counterweight, the lower boundary of the resonant area R1 was determined to be $n_{m,R1,LL}$=568 rpm, Fig. 19. Therefore, the value of $\Delta n_{m,R1}=n_{m,R1,V,UL,CWC}-n_{m,R1,V,LL,CWC}\approx 727-568=159$ rpm
is adopted as the real FREM width of the R1 resonant area from the standpoint of dynamic response. The remaining two resonances of the first order (R2 and R3) have a significant impact on the dynamic behavior of the superstructure.

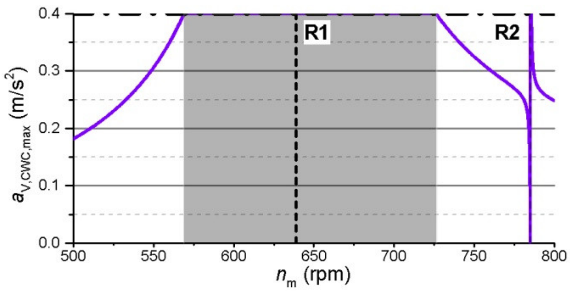

Figure 19. The FREM width of the resonant area R1 at the conditionally expanded span of the frequency regulation.

By overlapping the FREM domains where the partial limits of the dynamic response were satisfied, white zones presented in Figs. 4–15, it has been concluded that the criterion of permissible lateral accelerations allows for a wider FREM range, Figs. 20 and 21.

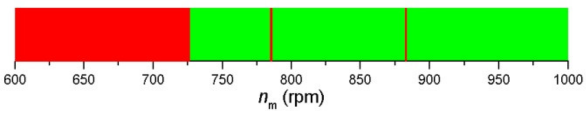

Figure 20. The FREM domains of the excessive (red) vs. permissible (green) vertical accelerations.

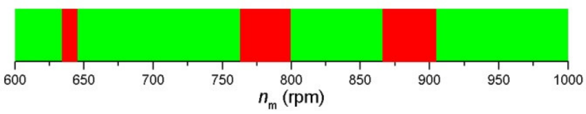

Figure 21. The FREM domains of the excessive (red) vs. permissible (green) lateral accelerations.

By overlapping the FREM resonant domains within the span of frequency regulation 600 rpm$\leq n_{EM}\leq$1000 rpm, Fig. 22, the existence of three resonant-free zones has been observed, Table 9.

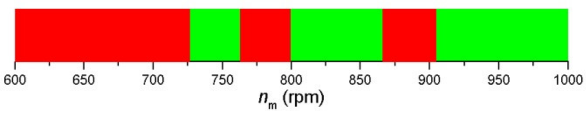

Figure 22. Resonant-free zones (green).

Table 9. The FREM boundaries and widths of the resonant-free zones (RFZs)

RFZ	Lower limit	Upper limit	Width
1	$n_{m,R1,UL}$=727 rpm	$n_{m,R2,LL}$=763 rpm	36 rpm
2	$n_{m,R2,UL}$=799 rpm	$n_{m,R3,LL}$=866 rpm	67 rpm
3	$n_{m,R3,UL}$=905 rpm	$n_{m,nom}$=1000 rpm	95 rpm

5. CONCLUSION

At this point in time, the primary role of the frequency-controlled drives of the working devices of continuous earthmoving machines is to protect the drive itself from being overloaded. The new idea of using frequency-controlled drives as a means of enabling the continuous earthmoving machines to overcome higher resistances to excavation while reducing or, if possible, completely avoiding the appearance of negative dynamic effects requires a detailed analysis of the dynamic response of the load-carrying structure in proximity to the potential resonant states. Defining of the ranges of the resonant states was performed on the basis of limiting accelerations of the referent points of the slewing superstructure of the bucket wheel excavator SchRs 1600 (which is a typical representative of the class of earthmoving machines exposed to the periodic excitation caused by the excavation process), prescribed by the German standard DIN 22261-2. This, however, should not be seen as a limitation or a downside of the presented method.

Based on the results of the presented studies, the following conclusions can be drawn:

- with the current number of buckets on the bucket wheel (17) and the range of frequencies of revolution of the bucket wheel drive electromotor (600 rpm to 1000 rpm, dictated by the parameters of the gearbox of the said drive), 3 potential resonant states of the slewing superstructure have been observed in the low-frequency range (up to 1.25 Hz);
- the criterion of limiting vertical accelerations fully defines the range (both the lower and the upper bounds) of one potential resonant state, whereas the criterion of limiting lateral accelerations fully defines the scope of the remaining 2 potential resonant states;
- the widest resonant area of the frequency of revolution of the bucket wheel drive electromotor (159 rpm), i.e. the highest sensitivity of the structure to the appearance of a resonance, occurs for the first order resonance exciting the first mode of the slewing superstructure, which is also the most dangerous case that must be avoided at all costs;
- the narrowest range of the resonant area of the frequency of revolution of the bucket wheel drive electromotor (2 rpm), i.e. the lowest sensitivity of the structure to the appearance of a resonance, occurs for the third order resonance which excites the sixth mode of the slewing superstructure;
- over the considered domain of the frequency of revolution of the bucket wheel drive electromotor (the width of 400 rpm), there are three resonant-free subdomains, the widest of which appears in the zone close to the nominal frequency of revolution of the bucket wheel drive electromotor (1000 rpm);
- within the working spectrum of the bucket wheel drive electromrotor (600 to 1000 rpm), a combined total of 50.5% (127 + 36 + 39 = 202 rpm) should be avoided, while a total of 49.5% (36 + 67 + 95 = 198 rpm) allows the machine to operate in the resonant-free areas.

Applying the presented method of analysis of the dynamic response makes it possible to establish the algorithms for controlling a system for soil excavation which would significantly lower the possibility of appearance of failures and breakdowns of the load-bearing structure and, therefore, very expensive standstills of this class of machines. Such algorithms could then be used to upgrade the system for controlling the working process and therefore prevent the load-bearing structure from entering the resonant states. In doing so, the reliance of proper operation of the machine of enormous importance and value on the operator's experience and ability to instantaneously assess the behavior of the system would be eliminated.

ACKNOWLEDGMENT

This work is a contribution to the Ministry of Education, Science and Technological Development of Serbia funded project "Integrated research in the fields of macro, micro and nano mechanical engineering" (Contract number: 451-03-68/2022-14/200105).

REFERENCES

[1] W. Durst, W. Vogt: *Bucket Wheel Excavator*, Trans Tech Publications, Clausthal-Zellerfeld, 1988.

[2] L. Rasper: *The bucket wheel excavator: Development, design, application*, Trans Tech Publications, Clausthal-Zellerfeld, 1975.

[3] D. Pietrusiak, P. Moczko, E. Rusiński: *World's largest movable mining machine vibration testing - numerical and experimental approach*, in: P. Sas, D. Moens, A. van de Walle (Eds.), Proceedings of International Conference on Noise and Vibration Engineering (ISMA2016) and International Conference on Uncertainty in Structural Dynamics (USD2016), Leuven (Belgium), 2016, Katholieke Universiteit Leuven, Haverlee (Belgium), pp. 2287–2299, 2016.

[4] E. Rusiński, J. Czmochowski, P. Moczko, D. Pietrusiak: *Surface mining machines - Problems of maintenance and modernization*, Springer International Publishing AG, Cham, 2017.

[5] I.C. Predoiu, D. Antonie, C.R. Pop, M.A. Teodorescu, S. Balacescu: *Current issues of the lignite deposit exploitation in Romania*, in: 24th World Mining Congress Proceedings–Mineral Exploration, Rio de Janeiro (Brazil), 2016, Brazilian Mining Association, Belo Horizonte (Brazil), pp. 30–38, 2016

[6] B.S. Dhillon: *Mining equipment reliability, maintainability, and safety*, Springer, London, 2008.

[7] M. Tanasijevic, D. Ivezic, D. Ignjatovic, D. Polovina: *Dependability as criteria for bucket wheel excavator revitalization*, J. Sci. Ind. Res. 70(1) (2011) 13–19.

[8] M. Tanasijević, D. Ivezić, P. Jovančić, D. Ćatić, D. Zlatanović: *Study of dependability evaluation for multi-hierarchical systems based on max-min composition*, Qual. Reliab. Eng. Int. 29, pp. 317–326, 2012.

[9] S. Kirin, A. Sedmak, W. Li, M. Brzaković, I. Miljanović, A. Petrović, S. Sedmak: *Human factor risk management procedures applied in the case of open pit mine*, Eng. Fail. Anal. 126, 105456, 2021.

[10] S. Djenadic, M. Tanasijevic, P. Jovancic, D. Ignjatovic, D. Petrovic, U. Bugaric: *Risk evaluation: Brief review and innovation model based on fuzzy logic and MCDM*, Mathematics-Basel, 10(5), 811, 2022.

[11] M. Pantelić, S. Bošnjak, M. Misita, N. Gnjatović, A. Stefanović: *Service FMECA of a bucket wheel excavator*, Eng. Fail. Anal. 108, 104289, 2020.

[12] U. Bugaric, M. Tanasijevic, D. Polovina, D. Ignjatovic, P. Jovancic: *Lost production costs of the overburden excavation system caused by rubber belt failure*, Eksploat. Niezawodn. 14(4), pp. 333–341, 2012.

[13] S. Bošnjak, N. Zrnić, V. Gašić, Z. Petković, A. Simonović: *External load variability of multibucket machines for mechanization*, Adv. Mater. Res-Switz. 422, pp. 678–683, 2012.

[14] M. Arsić, S Bošnjak, N. Zrnić, A. Sedmak, N. Gnjatović: *Bucket wheel failure caused by residual stresses in welded joints*, Eng. Fail. Anal. 18(2), pp. 700–712, 2011.

[15] A. Brkić, T. Maneski, D. Ignjatović, P. Jovančić, V. Spasojević Brkić: *Diagnostics of bucket wheel excavator discharge boom dynamic performance and its reconstruction*, Eksploat. Niezawodn. 16 (2), pp. 188–197, 2014.

[16] P. Jovančić, D. Ignjatović, M. Tanasijević, T. Maneski: *Load-bearing steel structure diagnostics on bucket wheel excavator, for the purpose of failure prevention*, Eng. Fail. Anal. 18(4), pp. 1203–1211, 2011.

[17] W. Huss: *Problems of bucket-wheel excavators body in hardly-workable grounds in Polish open pit mines*, in: C .Niemann-Delius (Eds.), Proceedings of the 12th International symposium continuous surface mining - Aachen (Germany), 2014, Lecture Notes in Production Engineering, Springer, Cham, pp. 59–71, 2015.

[18] S. Bošnjak, D. Oguamanam, N. Zrnić: *The influence of constructive parameters on response of bucket wheel excavator superstructure in the out-of-resonance region*, Arch. Civ. Mech. Eng. 15(4), pp. 977–985, 2015.

[19] E. Rusiński, P. Kaczyński, P. Moczko, D. Pietrusiak: *Bucket wheel excavator dynamics optimization on the stage of preliminary project*, Górnictwo Odkrywkowe 53(3-4), pp. 25–28, 2012.

[20] S. Bošnjak, Z. Petković, M. Đorđević, N. Gnjatović: *Redesign of the bucket wheel excavating device*, in: S. Bošnjak, N. Zrnić (Eds.), Proceedings of the 19th International conference on Material handling, constructions and logistics (MHCL '09), Belgrade (Serbia), 2009, University of Belgrade - Faculty of Mechanical Engineering, Belgrade, pp. 123–128, 2009.

[21] S. Bošnjak, N. Gnjatović, I. Milenović, A. Stefanović, M.Urošević: *Modernization and unification of the excavating devices of bucket wheel excavators SRs 2000 deployed in Serbian open pit mines*, in: G. Kartnig, N. Zrnić, S. Bošnjak (Eds.) Proceedings of the 23rd International conference on Material handling, constructions and logistics (MHCL 2019), Vienna (Austria), 2019, University of Belgrade - Faculty of Mechanical Engineering, Belgrade, pp. 175–182, 2019.

[22] DIN 22261-2: *Excavators, spreaders and auxiliary equipment in brown coal opencast lignite mines - Part 2: Calculation Principles* (in German), German Institute for Standardization, Berlin, 2016.

[23] AS4324.1: *Mobile equipment for continuous handling of bulk materials - Part 1: General requirements for the design of steel structures*, Standards Australia, Homebush (NSW), 2017.

[24] ISO 5049.: *Mobile Equipment for the Continuous Handling of Bulk Materials - Part 1: Rules for the Design of Steel Structures*, International Organization for Standardization, Geneva, 1994.

[25] P. Moczko, D. Pietrusiak, E. Rusiński: *Material handling and mining equipment - International standards, recommendations for design and testing*, FME Trans. 46 (3), pp. 291–298, 2018.

[26] N. Gnjatović, S. Bošnjak, I. Milenović, A. Stefanović: *Bucket wheel excavators: Dynamic response as a criterion for validation of the total number of buckets*, Eng. Struct. 225, 111313, 2020.

[27] N. Gnjatović, S. Bošnjak, A. Stefanović: *The dependency of the dynamic response of a two mast bucket wheel excavator superstructure on the counterweight mass and the degree of Fourier approximation of the digging resistance*, Arc. Min. Sci. 63(2), pp. 491–509, 2018.

[28] N. Gnjatović, S. Bošnjak, I. Milenović: *The influence of incrustation and chute blockage on the dynamic behaviour of a bucket wheel excavator slewing superstructure*, J. Theor. App. Mech-Pol. 58(3), 573–584, 2020.

[29] N. Gnjatović, S. Bošnjak, N. Zrnić; *Spatial reduced dynamic model of a bucket wheel excavator with two masts*, in: E. Rusiński, D. Pietrusiak, D. (Eds.), Proceedings of the 14^{th} International Scientific Conference: Computer Aided Engineering (CAE 2018), Wroclaw (Poland), 2018, Lecture Notes in Mechanical Engineering, Springer, Cham, pp. 215–235, 2019.

[30] S. Bošnjak, N. Gnjatović, *The influence of geometric configuration on response of the bucket wheel excavator superstructure*, FME Trans. 44(3), pp. 313–323, 2016.